

# Robust Radial Distortion from a Single Image

Faisal Bukhari and Matthew N. Dailey

Computer Science and Information Management  
Asian Institute of Technology  
Pathumthani, Thailand

**Abstract.** Many computer vision algorithms rely on the assumption of the pinhole camera model, but lens distortion with off-the-shelf cameras is significant enough to violate this assumption. Many methods for radial distortion estimation have been proposed, but they all have limitations. Robust automatic radial distortion estimation from a single natural image would be extremely useful for some applications. We propose a new method for radial distortion estimation based on the plumb-line approach. The method works from a single image and does not require a special calibration pattern. It is based on Fitzgibbon’s division model, robust estimation of circular arcs, and robust estimation of distortion parameters. In a series of experiments on synthetic and real images, we demonstrate the method’s ability to accurately identify distortion parameters and remove radial distortion from images.

## 1 Introduction

Most computer vision algorithms, particularly structure from motion algorithms, rely on the assumption of a linear pinhole camera model. However, most commercially available cameras introduce sufficiently severe optical distortion that the pinhole assumption is invalid, making distortion correction a must.

Radial distortion is the most significant type of distortion in today’s cameras [1, 2]. It is most evident in images produced with low-cost, wide-angle lenses. Such lenses are being widely deployed, for example, in automotive applications such as assisting drivers to view a vehicle’s blind spots [3, 4]. But it is also significant enough in higher-quality cameras to introduce error into 3D reconstruction processes. Radial distortion bends straight lines into circular arcs [2, 5], violating the main invariance preserved in the pinhole camera model, that straight lines in the world map to straight lines in the image plane [6, 7]. Radial distortion may appear as barrel distortion, usually arising at short focal lengths, or pincushion distortion, usually arising at longer focal lengths.

Methods for radial distortion estimation fall into three major categories: point correspondence [8, 1, 9], multiple view autocalibration [10–14], and plumb-line. Plumb-line methods are the most promising for robust distortion estimation from a single image or a small number of images. Rather than using a known pattern or sequence of images under camera motion, they estimate distortion parameters

directly from distorted straight lines in one or more images. Straight lines are frequent enough in most human-made environments to make distortion estimation from a single image possible [2, 5, 15]. However, existing methods require human intervention [16–18], do not use all available lines for distortion estimation despite the fact that additional lines could minimize estimation error [15, 2, 5], or assume the distortion center as the center of the image [2, 19], which is in contrast to recommendations [11, 20]. The Devernay and Faugeras [6] method is the only existing method that overcomes these limitations. However, it requires a complex process of polygonal approximation of the distorted lines. As we shall see, the distorted line detection process can be dramatically simplified by using an alternative distortion model.

In this paper, we propose a new method based on the plumb-line approach that addresses these limitations. The method works from a single image if the image contains a sufficient number of distorted straight lines. It does not require a calibration pattern or human intervention. We use Fitzgibbon’s division model of radial distortion [12] with a single parameter. Our estimator is similar to that of Strand and Hayman [2] and Wang et al. [5] in that we estimate the parameters of the distortion model from the parameters of circular arcs identified in the distorted image, based on the fact that distorted straight lines can be modeled as circular under the single parameter division model [10]. Our contribution is to make the process fully automatic and robust to outliers using a two-step random sampling process. For the first step, we introduce a sampling algorithm to search the input image for subsequences of contours that can be modeled as circular arcs. For the second step, we introduce a sampling algorithm that finds the distortion parameters consistent with the largest number of arcs. Based on these parameters, we undistort the input image.

To evaluate the new algorithm, we perform a quantitative study of its performance on distorted synthetic images and provide an example of its ability to remove distortion from a real image. We find that the algorithm performs very well, with excellent reconstruction of the original image even under severe distortion, and that it is able to eliminate the visible distortion in real images.

## 2 Mathematical Model

In this section, we outline the mathematical model of radial distortion assumed in the rest of the paper and show how to estimate the parameters of this model.

### 2.1 Distortion model

Although the most commonly used radial distortion model is the *even-order polynomial model*, we use Fitzgibbon’s *division model*, which is thought to be a more accurate approximation to the typical camera’s true distortion function:

$$x_u = \frac{x_d}{1 + \lambda_1 r_d^2 + \lambda_2 r_d^4 + \dots} \quad y_u = \frac{y_d}{1 + \lambda_1 r_d^2 + \lambda_2 r_d^4 + \dots} \quad .$$

$(x_u, y_u)$  and  $(x_d, y_d)$  are the corresponding coordinates of an undistorted point and a distorted point, respectively.  $r_d$  is the Euclidean distance of the distorted point to the distortion center; if the distortion center is the origin of the distorted image, we can write  $r_d^2 = x_d^2 + y_d^2$  or otherwise if  $(x_0, y_0)$  is the center, we write  $r_d^2 = (x_d - x_0)^2 + (y_d - y_0)^2$ .  $\lambda_1, \lambda_2, \lambda_3, \dots$  are the distortion parameters, which must be estimated from image measurements. We use the single parameter division model (fixing  $\lambda_2 = \lambda_3 = \dots = 0$ ), because for most cameras, a single term is sufficient [12, 5].

## 2.2 Distortion of a line under the single-parameter division model

Wang et al. [5] show that under the single-parameter division model, the distorted image of a straight line is a circular arc. However, they use the slope- $y$ -intercept form of the equation of a line, which we avoid due to its inability to model vertical lines and its undesirable numerical properties [21]. It can be shown (details omitted) that the general line

$$ax_u + by_u + c = 0 \quad (1)$$

is imaged as a circular arc on the circle

$$x_d^2 + y_d^2 + \frac{a}{c\lambda}x_d + \frac{b}{c\lambda}y_d + \frac{1}{\lambda} = 0, \quad (2)$$

under the single parameter division model. It is also possible to come to the same conclusion using the parametric form of a straight line [2]. When the distortion model includes a center of distortion that is not the image center, we obtain a more complex equation that still defines a circle.

## 2.3 Estimating distortion parameters from circular arcs

Strand and Hayman [2] and Wang et al. [5] show that it is possible to estimate  $\lambda$  from the parameters of circular arcs identified in an image. However, Rezazadegan and Reza [20] have found that modeling the distortion center in addition to the radial distortion parameter(s) can increase the accuracy of the calibration process. Wang et al. [5] thus further show how both  $\lambda$  and the distortion center (if not assumed to be the center of the image) can be estimated from the parameters of three circular arcs identified in an image. We use their formulation. For each arc  $i \in \{1, 2, 3\}$ , we rewrite Equation 2 in the form  $x_d^2 + y_d^2 + A_i x_d + B_i y_d + C_i = 0$ . Then the distortion center can be found by solving the linear system

$$\begin{aligned} (A_1 - A_2)x_0 + (B_1 - B_2)y_0 + (C_1 - C_2) &= 0 \\ (A_1 - A_3)x_0 + (B_1 - B_3)y_0 + (C_1 - C_3) &= 0 \\ (A_2 - A_3)x_0 + (B_2 - B_3)y_0 + (C_2 - C_3) &= 0, \end{aligned} \quad (3)$$

and  $\lambda$  can be estimated from

$$\frac{1}{\lambda} = x_0^2 + y_0^2 + Ax_0 + By_0 + C, \quad (4)$$

using any of the three circular arcs' parameters in place of  $(A, B, C)$ . See Wang et al. [5] for details.

### 3 Robust Radial Distortion Estimation

In this section, we provide the details of our approach, which is based on robust estimation and the mathematical model introduced in Section 2.

#### 3.1 Identifying circular arcs

The first step is to robustly identify as many circular arcs as possible in the image. Given an input image, we first extract Canny edges and link adjacent edge pixels into contours. We discard any contour whose length is below a threshold. For each remaining contour, we then attempt to find long pixel subsequences that can be fit by circular arcs. Our method is based on random sampling and inspired by RANSAC [22], but, rather than finding a single model for all the data, we preserve all models (candidate circular arcs) that are not overlapping with other arcs in the same contour that have more support. The termination criterion is to stop once the probability that an arc of minimal length has not yet been found is small. The detailed algorithm is presented in Section 3.5.

#### 3.2 Refining circular arc estimates

After the initial arc identification process is complete, each resulting arc, whose parameters have been calculated directly from the minimum sample of three points, is refined using the inlier pixel contour subsegment supporting that model. The gold standard objective function for circle fitting is

$$\Omega(x_c, y_c, r) = \sum_{i=1}^N d(x_i, y_i, x_c, y_c, r)^2, \quad (5)$$

where  $(x_c, y_c)$  is the center of the circle,  $r$  is its radius, and  $d(x, y, x_c, y_c, r)$  is the orthogonal distance of the measured point  $(x, y)$  to the hypothetical circle. Since there is no closed-form solution minimizing this objective function [23], we use an initial guess and the Levenberg-Marquardt nonlinear least squares method to find a local minimum.

As the initial estimate of the circle’s parameters, we use either the parameters calculated during the sampling procedure or Taubin’s method [24], which is based on algebraic error minimization.

#### 3.3 Estimating distortion parameters

Once we have obtained a set of circular arcs as candidate distorted straight lines, we use the estimator of Equations 3 and 4 and a standard RANSAC procedure to find a set of distortion parameters with maximal support. In the sampling loop, we sample three arcs, calculate the model, and count the number of arcs that are inliers by first undistorting them using the estimated distortion parameters then testing for straightness using orthogonal regression. The detailed algorithm is presented in Section 3.6.

**Require:** Contours  $C_1, C_2, \dots$   
**Ensure:**  $A$  is the output arc set

- 1:  $A \leftarrow \emptyset$
- 2: **for** each contour  $C_i$  **do**
- 3:   **if**  $|C_i| \geq l^{\min}$  **then**
- 4:      $N \leftarrow f(l^{\min}, |C_i|)$
- 5:     **for**  $n = 1$  to  $N$  **do**
- 6:       Sample three points  $\mathbf{x}_1, \mathbf{x}_2, \mathbf{x}_3$  from  $C_i$ .
- 7:       **if**  $\mathbf{x}_1, \mathbf{x}_2, \mathbf{x}_3$  are not collinear **then**
- 8:         Calculate  $x_c, y_c, r$  from  $\mathbf{x}_1, \mathbf{x}_2, \mathbf{x}_3$ .
- 9:          $A^{\text{new}} \leftarrow$  arc for longest subsequence of  $C_i$  consistent with  $x_c, y_c, r$
- 10:        **if**  $|A^{\text{new}}| \geq l^{\min}$  **then**
- 11:         **if**  $A^{\text{new}}$  does not overlap with any arc in  $A$  **then**
- 12:          $A \leftarrow A \cup \{A^{\text{new}}\}$
- 13:         **else if**  $A^{\text{new}}$  is longer than every overlapping arc in  $A$  **then**
- 14:         Remove arcs overlapping with  $A^{\text{new}}$  from  $A$
- 15:          $A \leftarrow A \cup \{A^{\text{new}}\}$
- 16:         **end if**
- 17:        **end if**
- 18:        **end if**
- 19:     **end for**
- 20:    **end if**
- 21: **end for**

**Algorithm 1:** Robust arc identification.

### 3.4 Undistortion

The last step in our procedure is to undistort the input image. We use the optimal distortion parameters and the inverse of the distortion model

$$x_d = x_0 + (1 + \lambda r_u^2)x_u \quad y_d = y_0 + (1 + \lambda r_u^2)y_u$$

with bilinear interpolation and appropriate translation and scale factors to produce the output undistorted image.

### 3.5 Robust arc identification algorithm

In Algorithm 1, we provide the details of our sampling-based arc identification method. To determine the number of iterations required, the algorithm uses a function  $f(l, n)$ , which gives the number of trials required to ensure that the probability of not sampling three of  $l$  inliers from a set of  $n$  points is small. This ensures that we sample a sufficient number of times to find, with high probability, all arcs with sufficient length in each contour.

### 3.6 Robust distortion parameter estimation algorithm

In Algorithm 2, we describe our estimation procedure in detail. Once a set of candidate arcs has been identified per Algorithm 1, distortion parameter estimation is a straightforward application of RANSAC [22]. In the sampling loop,

**Require:** Arc set  $A$   
**Ensure:**  $\lambda^*, x_0^*, y_0^*$  are the output distortion parameters

- 1:  $(\lambda^*, x_0^*, y_0^*) \leftarrow (\emptyset, \emptyset, \emptyset)$
- 2: **if**  $|A| \geq 3$  **then**
- 3:    $N \leftarrow 0$
- 4:    $s \leftarrow 0$
- 5:   **loop**
- 6:      $N \leftarrow N + 1$
- 7:     Sample three distinct arcs  $A_1, A_2, A_3$
- 8:     Estimate  $\lambda, x_0, y_0$  from  $A_1, A_2, A_3$  per Equations 3 and 4
- 9:     **if** support for  $(\lambda, x_0, y_0)$  is greater than  $s$  **then**
- 10:       $s \leftarrow$  support for  $(\lambda, x_0, y_0)$
- 11:       $(\lambda^*, x_0^*, y_0^*) \leftarrow (\lambda, x_0, y_0)$
- 12:     **end if**
- 13:     **if**  $N \geq f(s, |A|)$  **then**
- 14:      break
- 15:     **end if**
- 16:   **end loop**
- 17: **end if**

**Algorithm 2:** Robust distortion parameter estimation.

we use adaptive calculation of the number of iterations required based on the number of inlier arcs [7]. The termination criterion uses the same function  $f(l, n)$  to determine the number of trials required to ensure that the probability of not sampling three of  $l$  inliers from  $n$  items is small. An arc is judged to be an inlier if, after undistortion using the candidate distortion parameters  $\lambda, x_0$ , and  $y_0$ , the pixels of the arc form a straight line, as measured by orthogonal regression.

## 4 Experimental Evaluation

In this section, we describe a detailed quantitative study of the performance of our method on synthetic images and show qualitative results with real images. A sample of the images we used with results is shown in Fig. 1. We used the same original image (Fig. 1(a)) for all experiments. In each experiment, we distort the original image using particular ground truth values of  $\lambda, x_0$ , and  $y_0$  (Fig. 1(b)), identify circular arcs in the image (Fig. 1(c)), estimate the distortion parameters, and use those parameters to undistort the image (Fig. 1(d)).

We describe two series of experiments with synthetic images. In both cases, we used OpenCV’s Canny and contour extraction algorithms with a low gradient threshold of 50 and a high gradient threshold of 150. We fixed the minimum contour length at 150 pixels. For each contour of sufficient length, our arc extraction procedure (Algorithm 1) pre-calculates the number  $N$  of point sampling steps to perform using assuming a minimum number  $l^{\min} = 50$  of inlier pixels.

In a first series of runs, we varied  $\lambda$  while keeping the distortion center fixed at  $(x_0, y_0) = (320, 240)$ , the image center. In a second series of runs, we kept the distortion level fixed ( $\lambda = -10^{-6}$ ) while varying the distortion center. In every

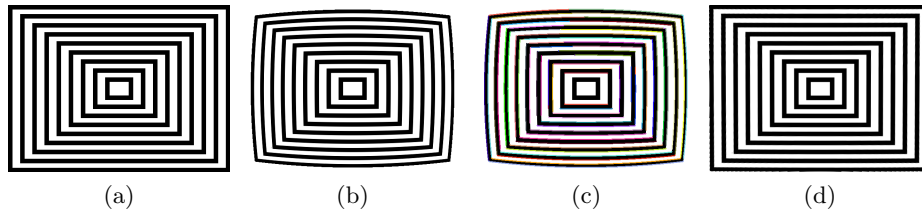


Fig. 1: Example experiment with synthetic image size  $640 \times 480$ . (a) Original image. (b) Distorted image with  $\lambda = -10^{-6}$ ,  $(x_0, y_0) = (320, 240)$  (the image center). (c) Estimated arcs. (d) Undistorted image using estimated values of  $\lambda = -9.8097^{-7}$ ,  $x_0 = 319.632$ , and  $y_0 = 247.75$ . Using true distortion parameters, RMSE = 3.74103 and using estimated parameters, RMSE = 3.79212.

case, we estimated all three parameters of the distortion model. We compare four methods for arc estimation. The results for varying  $\lambda$  are shown in Fig. 2, and the results for varying distortion center are shown in Fig. 3. The “Ransac” method means we accept the circular arc model computed from three sample points, without any refinement after calculating the inliers. “Ransac-Taubin” is the result of using the Taubin method to refine the arc model computed from three sample points. “Ransac-LM” is the result of applying the Levenberg-Marquardt method directly to the model computed from three sample points. Under the hypothesis that starting LM from the sample-based estimate might not work as well as an initial estimate closer to the optimum, we also performed one series of experiments in which we first applied the Taubin method to the sample-based model then applied LM to the Taubin estimate. The results from this method are shown as “Ransac-Taubin-LM.”

Over the two series of runs, we observe variability between the actual and estimated parameter values with all of the circle fitting methods, but the performance of the method in terms of RMSE is quite good. The “Ransac-LM” method provides the most stable performance over different levels of distortion and distortion center parameters. Even in the case of severe barrel distortion ( $\lambda = 10^{-5}$ ), the RMSE error introduced when undistorting using the parameters estimated by Ransac-LM is only about 30.06% more than that introduced when using the true distortion parameters.

Finally, in Fig. 4, we provide an example of the proposed method’s ability to identify distortion parameters and undistort a real image [25]. The robust arc selection and parameter estimation method is able to find a consensus set corresponding to distorted straight lines and is successful at removing most of the radial distortion from the image.

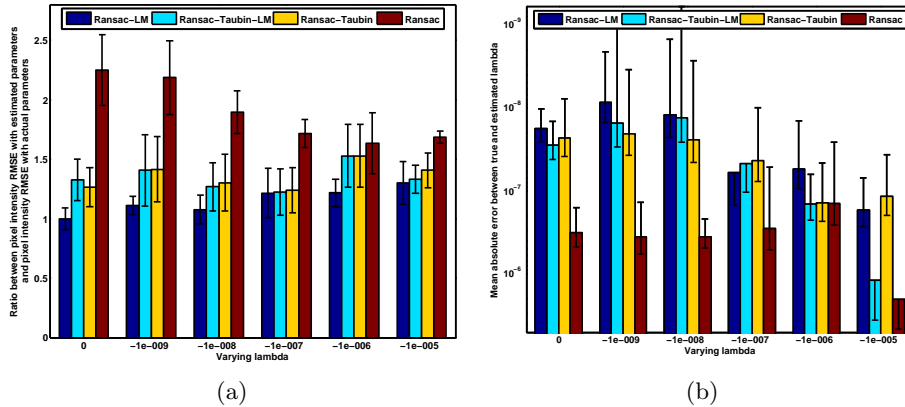


Fig. 2: Results of synthetic image experiments with varying  $\lambda$ . Distortion center is fixed at image center  $(x_0, y_0) = (320, 240)$ . (a) Noise in the undistorted image relative to the original image, measured by the ratio of the RMSE using estimated parameters to the RMSE using true parameters. (b) Error in estimating  $\lambda$ . Each point is an average over the same 10 runs shown in part (a). Each point is an average over 10 runs. Error bars denote 95% confidence intervals.

## 5 Conclusion

In this paper, we have introduced a new algorithm for radial distortion estimation and removal based on the plumb-line approach. The method works from a single image and does not require a special calibration pattern. It is based on Fitzgibbon’s division model, robust estimation of circular arcs, and robust estimation of distortion parameters. In a series of experiments on synthetic and real images, we have demonstrated the method’s ability to accurately identify distortion parameters and remove radial distortion from images.

The main limitation of the current implementation is that some parameters, especially the thresholds for Canny edge extraction, random sampling inlier calculations, and minimum contour length must be specified manually. In future work, we will improve the method to address these limitations.

## Acknowledgments

Faisal Bukhari was supported by a graduate fellowship from the Higher Education Commission of Pakistan. We are grateful to Irshad Ali for his valuable feedback and comments.

## References

1. Zhang, Z.: A flexible new technique for camera calibration. *IEEE Transactions on Pattern Analysis and Machine Intelligence* **22** (2000) 1330–1334

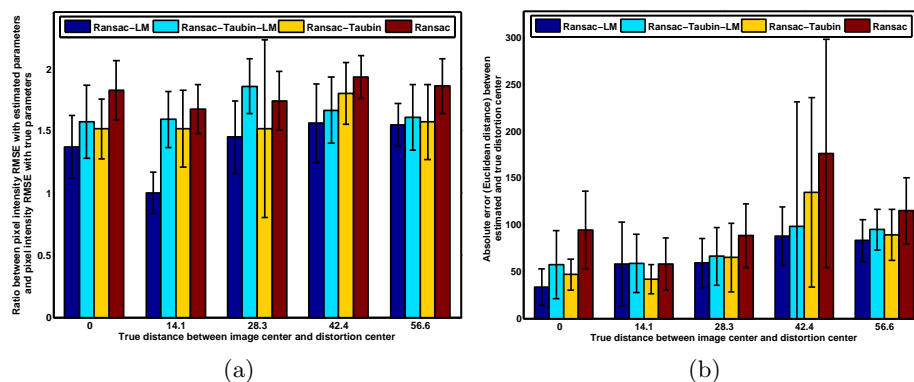


Fig. 3: Results of synthetic image experiments with varying distortion center. Distortion level is fixed at  $\lambda = -10^{-6}$ . (a) Noise in the undistorted image relative to the original image. (b) Error in estimating the distortion center. Each point is an average over 10 runs. Error bars denote 95% confidence intervals.

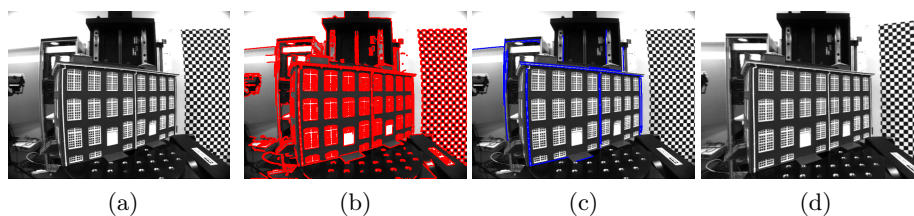


Fig. 4: Example results on real image. (a) Original image. (b) Extracted contours. (c) Identified arcs. (d) Undistorted image using parameters estimated via the “Ransac-LM” circle fitting method.

2. Strand, R., Hayman, E.: Correcting radial distortion by circle fitting. In: British Machine Vision Conference (BMVC). (2005)
3. Friel, M., Hughes, C., Denny, P., Jones, E., Glavin, M.: Automatic calibration of fish-eye cameras from automotive video sequences. *Intelligent Transport Systems, IET* **4** (2010) 136 – 148
4. Hughes, C., Glavin, M., Jones, E., Denny, P.: Wide-angle camera technology for automotive applications: a review. *Intelligent Transport Systems, IET* **3** (2009) 19 – 31
5. Wang, A., Qiu, T., Shao, L.: A simple method of radial distortion correction with centre of distortion estimation. *Journal of Mathematical Imaging and Vision* **35** (2009) 165–172
6. Devernay, F., Faugeras, O.: Straight lines have to be straight: Automatic calibration and removal of distortion from scenes of structured environments. *Machine Vision and Applications* **13** (2001) 14–24

7. Hartley, R., Zisserman, A.: *Multiple View Geometry in Computer Vision*. 2nd edn. Cambridge University Press (2004)
8. Tsai, R.Y.: A versatile camera calibration technique for high-accuracy 3D machine vision metrology using off-the-shelf TV cameras and lenses. *Radiometry* (1992) 221–244
9. Braüer-Burchardt, C.: A simple new method for precise lens distortion correction of low cost camera systems. In: *German Pattern Recognition Symposium*. (2004) 570–577
10. Barreto, J.P., Daniilidis, K.: Fundamental matrix for cameras with radial distortion. In: *International Conference on Computer Vision (ICCV)*. (2005) 625–632
11. Hartley, R., Kang, S.: Parameter-free radial distortion correction with center of distortion estimation. *IEEE Transactions on Pattern Analysis and Machine Intelligence* **29** (2007) 1309–1321
12. Fitzgibbon, A.W.: Simultaneous linear estimation of multiple view geometry and lens distortion. In: *IEEE International Conference on Computer Vision and Pattern Recognition (CVPR)*. (2001) 125–132
13. Stein, G.P.: Lens distortion calibration using point correspondences. In: *IEEE International Conference on Computer Vision and Pattern Recognition (CVPR)*. (1996) 602–608
14. Ramalingam, S., Sturm, P., Lodha, S.K.: Generic self-calibration of central cameras. *Computer Vision and Image Understanding* **114** (2010) 210–219
15. Thormählen, T., Broszio, H., Wassermann, I.: Robust line-based calibration of lens distortion from a single view. In: *Computer Vision / Computer Graphics Collaboration for Model-based Imaging Rendering, Image Analysis and Graphical Special Effects*. (2003) 105–112
16. Brown, D.C.: Close-range camera calibration. *Photogrammetric Engineering* **37** (1971) 855–866
17. Swaminathan, R., Nayar, S.: Non-Metric Calibration of Wide-Angle Lenses and Polycameras. *IEEE Transactions on Pattern Analysis and Machine Intelligence* **22** (2000) 1172 – 1178
18. Alvarez, L., Gómez, L., Sendra, J.R.: An algebraic approach to lens distortion by line rectification. *Journal of Mathematical Imaging and Vision* **35** (2009) 36–50
19. Brauer-Burchardt, C., Voss, K.: A new algorithm to correct fish-eye- and strong wide-angle-lens-distortion from single images. In: *IEEE International Conference on Image Processing*. Volume 1. (2001) 225 – 228
20. Tavakoli, H.R., Pourreza, H.R.: Automated center of radial distortion estimation, using active targets. In: *Asian Conference on Computer Vision (ACCV)*. (2010)
21. Chernov, N.: *Circular and Linear Regression: Fitting Circles and Lines by Least Squares*. Chapman & Hall (2010)
22. Fischler, M.A., Bolles, R.C.: Random sample consensus: a paradigm for model fitting with applications to image analysis and automated cartography. *Communications of the ACM* **24** (1981) 381–395
23. Al-Sharadqah, A., Chernov., N.: Error analysis for circle fitting algorithms. *The Electronic Journal of Statistics* **3** (2009) 886–911
24. Taubin, G.: Estimation of planar curves, surfaces, and nonplanar space curves defined by implicit equations with applications to edge and range image segmentation. *IEEE Transactions on Pattern Analysis and Machine Intelligence* **13** (1991) 1115–1138
25. Tomasi, C.: Sample image for CPS 296.1 homework assignment (2007) <http://www.cs.duke.edu/courses/spring06/cps296.1/homework/1/lab.gif>.